Available online at www.sciencedirect.com
ScienceDirect
Journal of Magnetism and Magnetic Materials 313 (2007) 236–242
www.elsevier.com/locate/jmmm

Comparison of magnetite nanocrystal formed by biomineralization and chemosynthesis

Lei Han, Shuangyan Li, Yong Yang, Fengmei Zhao, Jie Huang, Jin Chang*

Institute of Nanobiotechnology, School of Materials Science and Engineering, Tianjin University, Tianjin 300072, China

Received 3 September 2006; received in revised form 18 December 2006
Available online 17 January 2007

Abstract

Magnetite nanocrystal has been widely used in many fields. Recently, a new magnetite nanocrystal, called magnetosome, has been found in magnetotactic bacteria. In this article, we compared properties of magnetites prepared by co-precipitation with those of magnetosomes isolated from MSR-1 in detail, such as crystalline, morphology, crystal-size distributions, vitro cytotoxicity, and magnetic properties and quantified primary amino groups on the magnetosomes membrane surface by fluorescamine assay for the first time. From the results, it was clear that the magnetosomes might have potential in the biomedical applications in the future.

Keywords: Magnetosome; Synthetic magnetite; Magetotactic bacteria; Property

1. Introduction

Currently, there are few magnetic materials used as magnetic micro and nanocarriers in biomedical and biotechnological applications. Fe oxide and especially magnetite (Fe_3O_4), are mostly used in such applications, either as a background material for magnetic fluids or as magnetic particles, covered with a thin layer of polymer or other biocompatible materials [1]. Amorphous magnetic materials, both as micro and nanoparticles, could be successfully used as magnetic carriers because of their specific magnetic properties [2]. Recently, a new biologic magnetic nanomaterial, called magnetosome, was found in magnetotactic bacteria, which were first discovered by Blakemore [3]. The magnetosomes were small in size (40–120 nm) and dispersed very well because they were covered with a stable lipid membrane [4].

Magnetite prepared by co-precipitation, with the mean diameter smaller than 10 nm, was often used as the core of magnetic materials in the field of biomedicine for its superparamagnetic behavior and high saturation magnetization. On the other hand, the application of magnetosomes isolated from MSR-1 in the same field was researched widely. So, in this article, we compared the crystalline, morphology, crystal-size distributions, and magnetic properties of the magnetosome isolated from MSR-1 with those of magnetite prepared by co-precipitation. Furthermore, in order to connect magnetosomes with small biomolecule to serve as a new magnetic delivery system, we quantified the primary amino groups on its membrane by fluorescamine assay for the first time and compared vitro cytotoxicity of magnetosome with that of synthetic magnetite by MTT methods. These results showed that magnetosomes isolated from MSR-1 were suitable for being used as a new magnetic delivery system in the biomedical field in future.

2. Experimental

2.1. Materials

Magnetosomes, which were isolated from the cells of M. gryphiswaldense MSR-1, were presented by Microbiology Department, College of Biological Sciences, China Agricultural University [5,6]. Synthetic magnetites were prepared by co-precipitation in our lab [7,8]. Fluorescamine, Triton X-100, 3-[4,5-dimethylthiazol-2-yl]-2,5-diphenyltetrazolium bromide (MTT) and dimethylsulfoxide were

*Corresponding author. Tel.: +86 22 27401821; fax: +86 22 27401821.
E-mail address: jinchang@tju.edu.cn (J. Chang).

0304-8853/$ - see front matter © 2007 Elsevier B.V. All rights reserved.
doi:10.1016/j.jmmm.2007.01.004

purchased from sigma. Acetone was of spectroscopic grade (Merck). *O*-phosphorylethanolamine was purchased from Fluka. Borate buffer (pH = 8.25) was made at 50 mM concentration. All other chemicals were of analytical grade.

2.2. Analysis of crystalline phase

Crystalline phase identification of magnetosome and synthetic magnetite were carried out by X-ray diffraction (XRD) using a Rigaku D/max 2500 v/pc with Cu K_α radiations with a wavelength of $\lambda = 0.154056$ nm. The crystalline could be estimated from the full-width at half-maximum (FWHM) of the corresponding diffraction peaks.

2.3. Analysis of particle morphology

The morphologies of magnetosome and synthetic magnetite were observed using a JEOL-100CXII TEM operated at 200 kV. The TEM samples were prepared by deposition of a drop of magnetosome or synthetic magnetite nanoparticles precipitation solution onto a copper mesh grid covered with a carbon film.

2.4. Analysis of crystal-size distributions [9]

To quantify the crystal-size distributions of magnetosome and synthetic magnetite, we performed statistical analyses of particle size of them. Crystal outlines were digitized from scanned low-magnification TEM photomicrographs and their dimensions were estimated by calculating the best fit of an ellipse of same surface to the contour. The length (L) and width (W) of a crystal were then matched to the major and minor axes of the best-fitting ellipse, respectively. The particle sizes, reported in this article, were the averages of L and W. Although this ellipse-fitting method can introduce differences from actual measurement of L and W, the differences were checked and found to have negligible effects on the particle size distributions, even though the absolute mean values can differ somewhat from published results obtained with other methods.

2.5. Analysis of magnetic properties

Magnetic measurement of magnetosome and synthetic magnetite were performed by a vibrating sample magnetometer (VSM) from LakeShore Ltd. The samples were in the form of powder and were placed in Teflon sample holder. The magnetic measurements (hysteresis loops) were carried out in the field region of ± 1 T at room temperature. At 1 T, the magnetization of the samples was saturated.

2.6. Analysis of surface functional group [10,11]

2.6.1. Construction of standard curves

In order to quantify the amounts of primary amino groups in the magnetosome membrane and its outer surface, a standard curve, describing fluorescence intensity vs. total primary amino groups concentration was plotted. *O*-phosphorylethanolamine, used as standard material, was dissolved in borate buffer (pH = 8.25) at concentration of 3.64, 7.265, 10.90, 14.54, and 18.165 nmol/ml. At room temperature, fluorescamine solution (0.5 ml; 10 mg in 100 ml of acetone) was added to 500 μl of *O*-phosphorylethanolamine standard solution and then was shaken vigorously for 10 min. Then 1 ml of borate buffer was added to the sample followed by mixing for 20 min. All experiments were run three times. The resulting fluorescence was read within 1 h of reaction by exciting the sample at 390 nm and measuring the emitted radiation at 380 nm using a Hitachi F-4500 fluorimeter [12].

2.6.2. Determination of primary amino groups in outer magnetosome membrane

At room temperature, 0.40 mg magnetosomes were dispersed in 0.5 ml of borate buffer (pH = 8.25). Fluorescamine solution (0.5 ml; 10 mg in 100 ml of acetone) was added and the magnetosome sample solution was shaken vigorously for 10 min. Then 1 ml of 1.6% Triton X-100 in borate buffer was added to the sample followed by mixing for 20 min. All experiments were run three times. The sample was read as described above.

2.6.3. Determination of total primary amino groups in magnetosome membrane

At room temperature, 0.40 mg of magnetosomes were disrupted with 1.0 ml of 1.6% Triton X-100 in borate buffer (pH = 8.25) for 20 min. Fluorescamine solution (0.5 ml) was added and the magnetosome sample was shaken vigorously for 10 min. Then, 0.5 ml of borate buffer was added to the sample followed by mixing. All experiments were run three times. The sample was read as described above.

2.7. Analysis of cell toxicity

The MTT assay is a simple colorimetric assay to measure cell cytotoxicity, proliferation or viability [13]. Magnetosomes and synthetic magnetites were sterilized by γ-ray radiation and dispersed in serum supplemented tissue culture medium. L929 cells were plated into 96-well culture plates at a density of 5.0×10^3 cells/well. After incubation in a humidified 5% CO_2 incubator at 37 °C for 24 h, culture medium was replaced by 100 μl serial dilutions of the magnetosome and synthetic magnetite and the cells were incubated for 24, 48, and 72 h. After 24, 48, 72 h of incubation, 15 μl of MTT solution (5 mg/ml) was added to each well and allowed to incubate for further 4 h. Since living cells metabolized the MTT in their mitochondria and formed blue formazan crystals, 150 μl of dimethylsulfoxide was added to each well to dissolve the crystals thus formed. The wells were measured spectrophotometrically in an ELISA plate reader (Thermo Labsystems Multiskan MK3) at a wavelength of 560 nm (test). The spectrophotometrical

value of wells using culture medium-free solution was calibrated to zero. All experiments were run eight times. The relative cell viability (%) related to control wells containing cell culture medium without magnetosomes and synthetic magnetites was calculated by [A]test/[A]control × 100. Through the protocol, the cell viability of synthetic magnetites and magnetosomes particles were measured [14].

3. Results and discussion

3.1. Analysis of crystalline phase

As shown in Fig. 1, the XRD powder diffraction peaks of synthetic magnetic nanocrystal- and magnetosome-matched well with the standard Fe_3O_4 reflections. Thus, we can confirm that both magnetic nanocrystal within the magnetosome and synthetic magnetic nanocrystal are consisted of magnetites. It was well known that the FWHM of XRD pattern reflected crystallinity of the samples. Narrower the FWHM was, the higher crystallinity the sample was [15]. As shown in Table 1, both synthetic magnetite and magnetosome had perfect crystallinity for their narrow FWHM. At the same time, the FWHM of magnetosome XRD pattern were all smaller than that of synthetic magnetite in all diffraction direction. Thus, it can be drawn that magnetosome synthesized by biomineralization had higher crystallinity than synthetic magnetite.

3.2. Analysis of particle morphology

Electron micrographs of the magnetosomes reveal that magnetosomes dispersed very well and are often arranged in bent chains (Fig. 2a) which tend to form closed loops

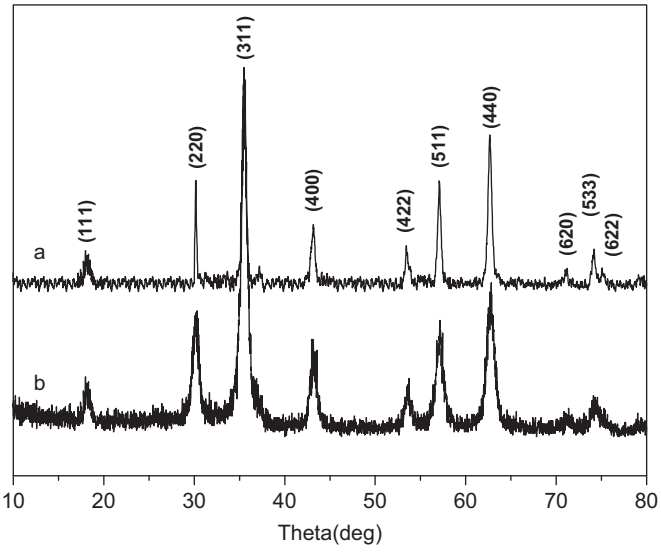

Fig. 1. XRD diffraction patterns of magnetosomes (a) and synthetic magnetite (b).

Table 1
FWHM of XRD pattern comparison of magnetosome and synthetic magnetite

	(111)	(220)	(311)	(400)	(422)	(511)	(440)	(533)
Magnetosome	0.282	0.306	0.471	0.353	0.235	0.329	0.424	0.353
Magnetite	0.696	0.736	0.785	0.776	0.724	0.773	1.010	0.875

(Fig.2b) in suspension so as to minimize their magnetic stray field energy [16]. The reason for this phenomenon is that the existing lipid membrane (Fig. .2c) surrounding magnetic core prevents them from completely sticking together by electrostatic repulsion and imparted flexibility to them [17]. As was stated by Valeri [18], elasticity may play a major role in the magnetosome arrangement of bent configurations. Thus, if not being surrounded by anything, there is obvious tendency of clustering for synthetic magnetites in most cases (Fig. 2d).

3.3. Analysis of crystal-size distributions

We measured the dimensions of 100 magnetosomes and 100 synthetic magnetites and plotted their frequencies as a function of particle size as shown in Fig. 3. The particle size of the synthetic magnetites varied from 7 to 18 nm, with the maximum of the size distribution at 9–12 nm. Therefore, synthetic magnetite particles are mostly in the superparamagnetic size domain. And the particle size of the magnetosomes varies from 10 to 60 nm, with the maximum of the size distribution at 40–50 nm, and thus belongs into the single magnetic domain (SD) range [19].

In agreement with previous results [20,21], the crystal-size distributions (CSDs) curves of magnetosomes were asymmetric and negatively skewed with sharp cut-offs toward larger sizes (Fig. 3b). This was due to the strict control of biomineralization by bacteria, in which the magnetosomes stopped growing once they reached a certain, strain-specific size. On the contrary, the CSDs of synthetic magnetites were a log-normal distribution, but with sharp cut-offs toward smaller sizes (Fig. 3a)[22]. Kile et al. [23] associated log-normal CSDs with decaying rate of nucleation accompanied by surface-controlled growth. The oppositely asymmetric distributions from synthetic magnetite and magnetosome thus might provide the robust potential criterion for distinguishing biogenic from synthetic magnetites.

3.4. Analysis of magnetic properties

Fig. 4 shows the magnetization (M) vs. field (H) curve at 300 K for samples of magnetosome and synthetic magnetite. From the curve of synthetic magnetite, it was observed that synthetic magnetite had no remanence and no coercivity and showed superparamagnetic bahavior. But the curve of magnetosomes exhibited ferromagnetic

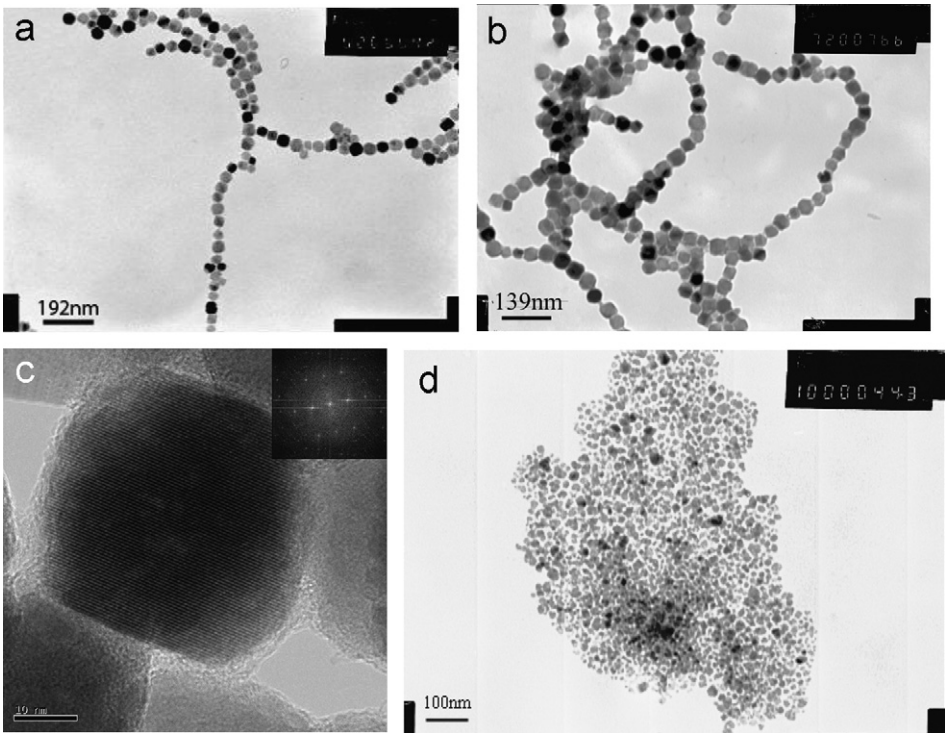

Fig. 2. TEM images of the magnetosomes (a) (b) and synthetic magnetites (d). HRTEM and Fourier transform of magnetosome (c).

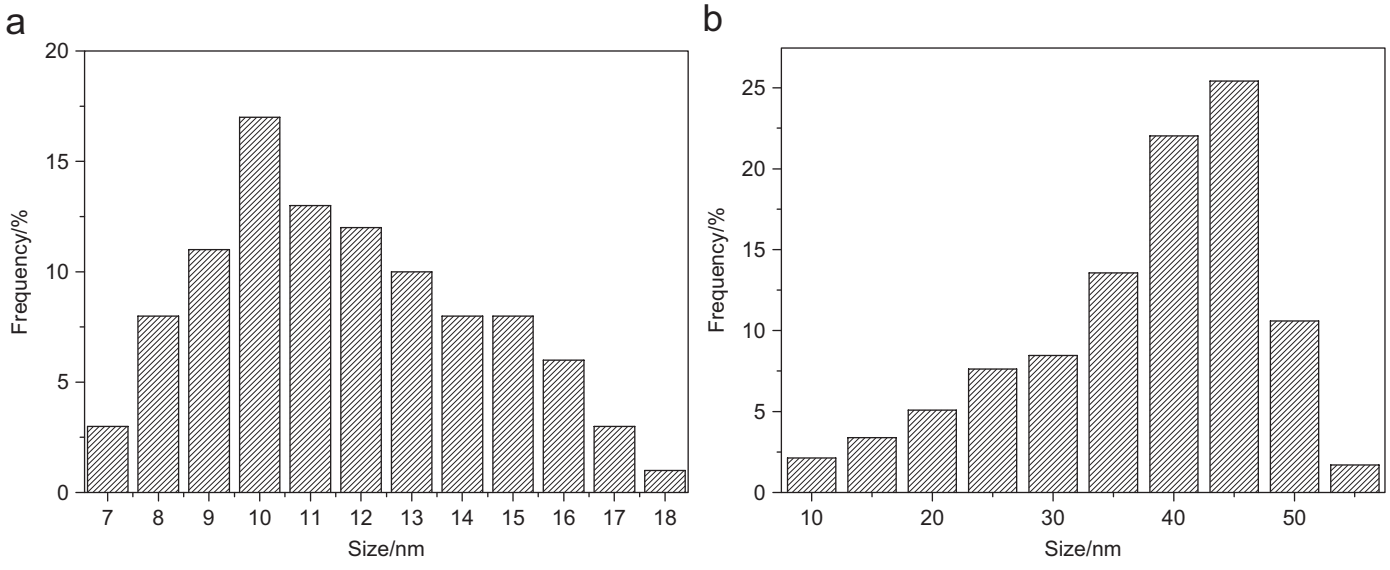

Fig. 3. Distinctly different crystal-size distribution curves of (a) synthetic magnetite and (b) magnetosome.

behavior with a coercivity of 75 Oe and remanence of 10 emu/g. It is that, for ultrafine magnetically ordered magnetite particles, the transition from superparamagnetic to ferromagnetic behavior occurs at a critical size D_p of 25 nm [24]. Thus, synthetic magnetites are superparamagnetic because their mean size (10 nm) is smaller than the D_p and the magnetosomes are ferromagnetic because their mean size (45 nm) is larger than the D_p.

The saturation magnetization of the synthetic magnetites, 72 emu/g, is larger than that of magnetosomes, 60 emu/g in the field region of ± 1 T at 300 K. This was due to the presence of nonmagnetic lipid membrane of 3–5 nm thickness in the outer of magnetosomes [25]. At the same time, the results showed that both magnetosomes and synthetic magnetites had high magnetic response due to their perfect crystallinity.

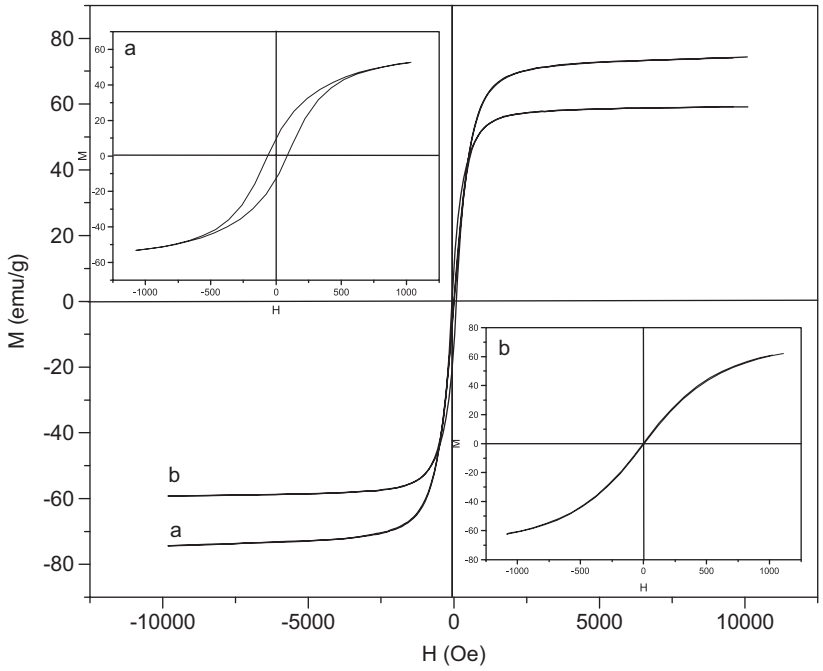

Fig. 4. Magnetization curve of magnetosome (a) and synthetic magnetite (b) obtained by VSM.

3.5. Analysis of surface functional group

As we all know, there were only hydroxyl groups in the surface of synthetic magnetite [26]. So it is difficult to connect the synthetic magnetites with other small biomolecules, such as antibody, enzyme, polypeptide, and so on.

On the contrary, magnetosome was known to be surrounded by special lipids membrane and some protein that is thought to be responsible for the biomineralization, morphologies, and sizes of the nanocrystals [27]. Lipids membrane contained the following three parts: (I) neutral lipids and free fatty acids, (II) glycolipids and sulfolipids, and (III) phospholipids (in weight ratio of 1:4:6). Phospholipids included phosphatidylserine and phosphatidylethanolamine (PE) [28,29]. Therefore, there were some amino and carboxyl groups on the surface of the magnetosome membrane. It was very convenient to connect magnetosomes with other small biomolecules by these groups [30,31]. So quantifying the amounts of these groups seemed to be very important. But, up to now, we do not find any articles quantifying the functional groups in the magnetosome surface. In this article, primary amino groups in the surface of magnetosomes were quantified by fluorescamine assay for the first time [32].

The first stage of this investigation was aimed at establishing the standard curves describing the fluorescamine intensity vs. the concentration of standard material for assaying transmembrane distributions of the primary amino groups in lipid membrane of magnetosome and quantifying primary amino groups in the surface of magnetosome membrane .We checked the linearity of fluorescence intensity between the range from 3.64 to

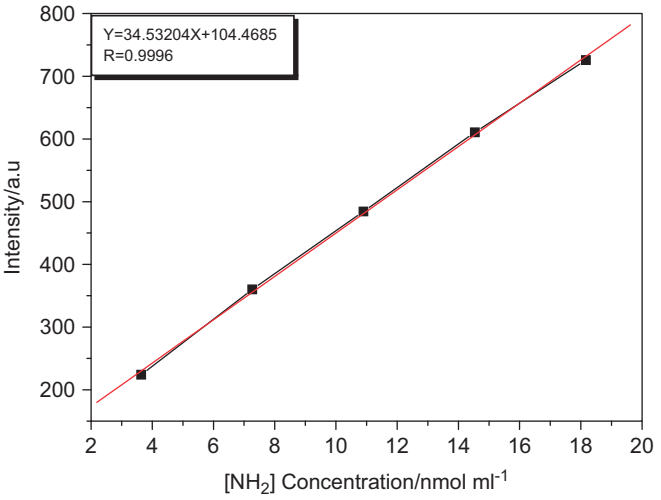

Fig. 5. Standard curves for the reaction of fluorescamine with *O*-phosphorylethanolamine. Fluorescence intensity is plotted vs. total primary amino concentration.

18.165 nmol/ml of *O*-phosphorylethanolamine, as shown in Fig. 5. In this assay, a solution gave mean values of 464.062 (arbitrary units of fluorescence) ($n = 3$) when it was assayed as external primary amino groups and 510.914 ($n = 3$) for total primary amino groups. A comparison of the two mean values showed that 90% of total primary amino groups were distributed in external lipid membrane [33]. Compared with the standard curves, the primary amino groups in the external membrane of magnetosomes are 52.73 nmol/mg.

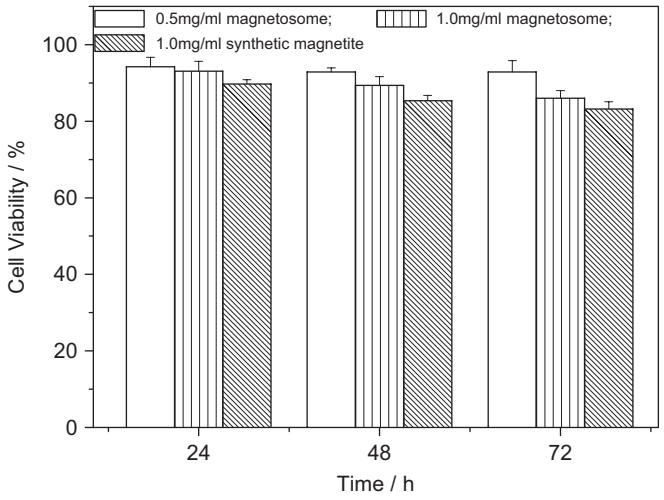

Fig. 6. Effect of magnetosome and synthetic magnetite on L929 cell viability measured by MTT assay after 24, 48, and 72 h incubation at 37 °C. Each value represents the mean ± SD of eight determinations.

3.6. Analysis of vitro cytotoxicity

MTT test was used to determine effects of the synthetic and biogenic magnetites on metabolic activity. As shown in Fig. 6, both synthetic and biogenic magnetite affected the metabolic activity in a concentration- and time-dependent manner when they were incubated with L929 cells in the concentration range 0.5–1.0 mg/ml for 24 to 72 h. It was clear that the cytotoxicity of the synthetic and biogenic magnetites decreased in relation to decreased concentration and incubation time. After 72 h, we determined more than 85% viable cells after incubation with synthetic magnetites at 1.0 mg/ml. However, incubation with magnetosomes at 1.0 mg/ml after 72 h showed that the viability of cells just reduced to 90%.

As we know, the cytotoxicity of nanomaterial is thought to be the result of the interaction between positive charge on nanomaterial surfaces and negative charge on cell surfaces [34]. Because of existing lipid membrane with negative charge on the magnetosomes surface and only some hydroxyl groups on the synthetic magnetites surface, weak interaction between them and cells surface led to their low cytotoxicity [35]. At the same time, lipid membrane on magnetosomes surface endowed them with better biocompatibility than synthetic magnetites.

4. Conclusion

In this study, through the XRD assay, it was shown that the magnetic core of magnetosomes was consisted of magnetite with better crystallographic performance than synthetic magnetites. Then, by analysis of particle morphology and crystal-size distributions, we confirm the potential criterion for distinguishing biogenic from synthetic magnetites. Furthermore, we quantified the amounts of the primary amino groups in the surface of the magnetosome membrane and its transmembrane distributions through fluorescamine assay for the first time. Finally, the MTT assay showed that magnetosomes had better biocompatibility than synthetic magnetites. All these better properties of magnetosomes isolated from MSR-1 suggested it might be widely used in biomedical fields as the synthetic magnetite in the future.

Acknowledgments

This work was supported by National Natural Science Foundation of China (No. 50373033) and Key Project Foundation from Tianjin Science and Technology Committee (No. 05YFJZJC01001), to which the authors wish to express their thanks.

References

[1] W. Moller, K. Scheuch, J. Sommer, J. Magn. Magn. Mater. 225 (2001) 8.
[2] H. Chiriac, A.E. Moga, G. Iacob, J. Magn. Magn. Mater. 293 (2005) 28.
[3] R.P. Blakemore, Science 190 (1975) 377.
[4] N. Nakamura, J.G. Burgess, K. Yagiuda, Anal. Chem. 65 (1993) 2036.
[5] W. Jiang, J.B. Sun, Y. Li, China J. Mod. Med. 15 (2005) 3521.
[6] W. Jiang, D.H. Zhao, Y. Li, Chinese Sci. Bull. 47 (2002) 1722.
[7] G. Xie, Q.Y. Zhang, Z.P. Luo, J. Appl. Polym. Sci. 87 (2003) 1733.
[8] A.J. Zhao, P. Yao, C.S. Kang, J. Magn. Magn. Mater. 295 (2005) 37.
[9] B. Devouard, M. Posfai, X. Hua, Am. Miner. 83 (1998) 1387.
[10] M.T. Roy, M. Gallardo, J. Estelrich, Bioconjugate Chem. 8 (1997) 941.
[11] E. Tavemier, A. Pugin, Biochimie 77 (1995) 174.
[12] S. Udenfriend, S. Stein, P. Bohlen, Science 178 (1972) 871.
[13] D.H. Kim, S.H. Lee, K.N. Kim, J. Magn. Magn. Mater. 293 (2005) 287.
[14] D. Fischer, Y. Li, B. Ahlemeyer, Biomaterials 24 (2003) 1121.
[15] D. Sudfeld, I. Ennen, A. Hutten, J. Magn. Magn. Mater. 293 (2005) 151.
[16] R. Hert, R. Hiergeist, M. Zeisberger, J. Magn. Magn. Mater. 293 (2005) 80.
[17] D. Schuler, R.B. Frankel, Appl. Microbiol. Biotechnol. 52 (1999) 464.
[18] P. Valeri, Shcherbakov, M. Winklhofer, Eur. Biophys. J. 26 (1997) 319.
[19] Y. Bao, K.M. Krishnan, J. Magn. Magn. Mater. 293 (2005) 15.
[20] B. Arato, Z. Szanyi, C. Flies, Am. Miner. 90 (2005) 1233.
[21] M. Posfai, K. Cziner, E. Marton, Eur. Biophys. J. 13 (2001) 691.
[22] D. Faivre, N. Menguy, F. Guyot, Am. Miner. 90 (2005) 1793.
[23] D.E. Kile, D.D. Eberl, A.R. Hoch, Geochim. Cosmochim. Acta 64 (2000) 2937.
[24] N.H. Hai, R. Lemoine, S. Remboldt, J. Magn. Magn. Mater. 293 (2005) 75.
[25] A. Hoell, A. Wiedenmann, U. Heyen, Physica B 350 (2004) 309.
[26] F. Gao, B.F. Pan, W.M. Zheng, J. Magn. Magn. Mater. 293 (2005) 48.
[27] T. Matsunaga, Y. Okamura, Trends Microbiol. 11 (2003) 536.
[28] Y.A. Gorby, T.J. Beveridge, R.P. Blakemore, J. Bacteriol. 170 (1988) 834.
[29] K. Grunberg, E.C. Muller, A. Otto, Appl. Environ. Microbiol. 70 (2004) 1040.

[30] N. Nakamura, K. Hashimoto, T. Matsunaga, Anal. Chem. 63 (1991) 268.
[31] T. Matsunaga, R. Sato, S. Kamiya, J. Magn. Magn. Mater. 194 (1999) 126.
[32] H.C. Lee, J. Forte, Biochim. Biophys. Acta 554 (1979) 375.
[33] S. Wieland, R. Schubert, R. Peschka, J. Liposome Res. 9 (1999) 477.
[34] R. Jevprasesphant, J. Penny, R. Jalal, Int. J. Pharm. 252 (2003) 263.
[35] T. Tanaka, T. Matsunaga, Anal.Chem. 72 (2000) 3518.